Environmental Engineering and Management Journal

June 2024, Vol. 23, No. 6, 1247-1257
http://www.eemj.icpm.tuiasi.ro/; http://www.eemj.eu
http://doi.org/10.30638/eemj.2024.101

"Gheorghe Asachi" Technical University of Iasi, Romania

A COMPARATIVE STUDY OF THE SEBAL ALGORITHM AND SWAP MODEL FOR EVAPOTRANSPIRATION RATE ESTIMATION IN QAZVIN PROVINCE, IRAN

Mahsa Hojabri, Majid Vazifedoust, Afshin Ashrafzadeh*

Department of Water Engineering, Faculty of Agricultural Sciences, University of Guilan, Rasht, Iran

Abstract

Given the significance of remote sensing for evapotranspiration (ET) estimation on a regional scale, this research seeks to assess actual ET (ETa) data derived from the Surface Energy Balance Algorithm for Land (SEBAL) algorithm, employing ground-based data as a reference point. The study focused on two corn fields in Qazvin province of Iran, where the Soil Water Atmosphere Plant (SWAP) model underwent calibration using observed soil water content data. The performance of SWAP in estimating soil water content was acceptable, with error measures indicating a normalized Root Mean Square Error (nRMSE) of 14.4% for the 0-15 cm soil layer and 12.6% for the 15-30 cm soil layer. ETa estimates extracted from the calibrated SWAP were considered as the benchmark. Comparing SEBAL's ETa estimates with those from SWAP reveals a linear relationship (R^2 = 0.67), and the error associated with SEBAL estimates is interpreted as low, with an RMSE of 2.3 mm/d. However, SEBAL consistently tends to underestimate ETa values. This study demonstrates that ETa data obtained through remote sensing, characterized by superior spatial and temporal resolution compared to ground-based data, can be reliably utilized in the irrigation planning of agricultural fields within the study area.

Key words: evapotranspiration rate, Qazvin province, SEBAL, SWAP

Received: May, 2023; Revised final: February, 2024; Accepted: February, 2024; Published in final edited form: June, 2024

1. Introduction

Evapotranspiration (ET) estimation is essential in various fields, including agriculture, hydrology, and environmental science, as it directly impacts water availability (Ghiat et al., 2021). The quantification of ET poses a significant research challenge in hydrology due to substantial spatio-temporal variability (especially in arid and semi-arid regions) and challenges related to data acquisition (Gebremedhin et al., 2022). Recent studies, such as Wu et al. (2020) and Giles-Hansen and Wei (2021), highlight that regional-scale ET estimation involves integrating multi-source satellite data and dynamic models. This approach provides a comprehensive view of ET across diverse landscapes, aiding water resource management and ecosystem understanding. Prior to the utilization of satellite data, estimating ET rates was limited to discrete locations with meteorological data. However, with advancements in technology, particularly remote sensing, contemporary methods enable the derivation of regional ET estimates (Li et al., 2009; Monteiro dos Reis et al., 2022).

Regional estimates of evaporation rates from water bodies and ET rates can help improve water resources management in watersheds and agricultural fields (Wanniarachchi and Sarukkalige, 2022). Remote sensing-based ET monitoring can also provide farmers with helpful information to improve irrigation scheduling. Continuous monitoring of ET through remote sensing equips farmers with real-time information about crop water requirements,

* Author to whom all correspondence should be addressed: e-mail ashrafzadeh@guilan.ac.ir

facilitating precision irrigation practices tailored to specific environmental conditions and crop needs. This crucial information enhances the efficiency of water resource management in agriculture (Foster et al., 2020). Over the past twenty years, there has been the emergence of algorithms, including Surface Energy Balance Algorithm for Land (SEBAL) (Bastiaanssen et al., 1998a; 1998b), Surface Energy Balance System (SEBS) (Su, 2002), Mapping ET at high Resolution using Internalized Calibration (METRIC) (Allen et al., 2005), Two-Source Energy Budget (TSEB) (Norman et al., 1995), and Atmosphere-Land EXchange Inverse (ALEXI) (Anderson et al., 1997), which leverage satellite data and the surface energy balance equation to estimate regional ET rates.

Among various algorithms for estimating evapotranspiration, SEBAL stands out for its widespread application and consistent assessment in diverse geographical regions (Ma et al., 2023). However, even though SEBAL has a potent theoretical framework, its complexity, and many parameters are considered its main drawbacks (Zhou et al., 2014). Previous studies collectively suggest that, depending on climatic and meteorological conditions and considering the properties of land cover types, the accuracy of SEBAL in estimating ET rates ranges from 67% to 97% (Paul et al., 2013). So, before using SEBAL in a specific study area, it could be helpful to evaluate its performance and assess the accuracy of estimates provided by the algorithm. Ground truth data of ET rates have been utilized as benchmarks to evaluate the performance of algorithms that derive ET products from satellite data. These data can be acquired from various instruments, including weighing lysimeters, Eddy Covariance (EC) systems, and Large Aperture Scintillometers (LASs), which range in complexity. Paul et al. (2013), using observed data from four large weighing lysimeters located in cotton fields, assessed the SEBAL algorithm. They found an overall bias of 28.2% between satellite-based and observed ET rates. Zhou et al. (2014) reported that, on average, SEBAL estimates of ET rates are 4% higher than the estimates obtained from the eddy covariance system they used in their study. Obtaining sufficient and accurate ground-based data for validating satellite-based estimates of ET rates is often challenging, and using instruments such as eddy covariance systems or scintillometers can require significant effort. As a result, some researchers turn to alternative data sources, such as pan evaporation data (e.g., Sun et al., 2011) or actual ET (ETa) rates derived from field-scale moisture flow models (e.g., Minacapilli et al., 2009), to validate these estimates.

This study aims to validate ET rates derived from the SEBAL algorithm using field-measured data from two corn fields in northern Iran. To achieve this, the Soil-Water-Atmosphere-Plant (SWAP) model has been implemented and calibrated based on soil water content measurements. The calibrated model's ETa estimates are then compared with those produced by the SEBAL algorithm. By conducting this comparison, the study assesses the accuracy of SEBAL's remote sensing-based estimates, specifically in the corn fields under investigation. This approach contributes to validating satellite-based ET estimates and enhances their reliability for applications in water resource management.

SWAP's effectiveness is evident in its outperformance during wet conditions, as highlighted by Kim et al. (2015). The model's ability to provide accurate soil moisture estimates underlines its strength, particularly in scenarios where other models may falter. Gandolfi et al. (2006) explored comparisons between different water flow models. These studies shed light on the strengths and limitations of various models, contributing to the ongoing discussion on selecting the most suitable model for specific conditions.

In-depth analyses, including Strengths, Weaknesses, Opportunities, and Threats (SWOT) assessments, have been conducted to evaluate one- and multi-dimensional soil water flow models based on the Richards equation, as presented by van Dam et al. (2004). These assessments comprehensively understand these models' conceptual and mathematical underpinnings. In summary, the continuous exploration and refinement of soil water flow models, exemplified by SWAP, contribute to advancing our understanding of soil-water dynamics, providing valuable tools for hydrological research. Despite its strengths, the model faces challenges in handling seasonal variations, spatial limitations, and complex calibration processes, particularly under deficit irrigation conditions. Understanding these aspects is crucial for the informed interpretation and application of the SWAP model outputs in agriculture and water resource management.

The present study addresses the growing need for accurate ETa estimation using satellite data, emphasizing its applicability in monitoring large-scale industrial farms and optimizing water resource management practices in agriculture. However, despite the indispensability and utility of satellite-based data, their accuracy needs validation through ground-based and precise measurements. In this study, the ETa extracted from the calibrated SWAP model served as a benchmark to assess the data provided by SEBAL. Once the satellite data is rigorously assessed and confirmed, it can be effectively utilized, leveraging its high spatial and temporal resolution advantages.

2. Materials and method

2.1. Study area

The present study was conducted at the Hezar-Jolfa Agro-Industrial Complex in the northern Iranian province of Qazvin. Covering a total land area of 15,567 km^2, mainly dedicated to agriculture, the Qazvin province is a leading agricultural production zone in Iran (Faraji et al., 2017). According to the Köppen-Geiger climate classification system (Kottek

et al., 2006), the climate of Qazvin Province is cold semi-arid (steppe) or BSk (B; arid; S: steppe; k: cold). The Hezar-Jolfa Complex encompasses an area of 860 ha and contains agricultural fields of different sizes, mainly cultivated for wheat, barley, sugar beet, and corn. Two separate corn fields (namely CP2 and CP5) - 38.9 ha and 45.6 ha, both irrigated by a center pivot sprinkler irrigation system — were chosen for the present study. During the summer cropping season of 2012 (from June 25 to October 15), a study by Fallah (2014) involved dividing the central portion of each field into four equally sized square subsections. Within these subsections, soil water content measurements were taken at four randomly selected locations. The measurements were conducted at two depths (0-15 cm and 15-30 cm). Fig. 1 illustrates the study area's location in Iran, an aerial photograph of the two fields being examined, and the positions of the measuring subsections within each field.

2.2. The SWAP Model

The SWAP model is based on the physical relationship among Soil, Water, Atmosphere, and Plant and simulates plant growth and the processes of flow, solute, and heat transport in soil. SWAP can estimate the temporal and spatial variations of soil moisture and ET, which are the main components of the soil water balance equation. The SWAP model is frequently used worldwide for assessing irrigation scenarios, simulating and managing saline soils, estimating water table variations, forecasting plant production, and estimating variables such as soil water content (Badiehneshin et al., 2015; Bennett et al., 2013; Hassanli et al., 2016; Kumar et al., 2015; Ma et al., 2015;Noory et al., 2011; ;). SWAP employs numerical solutions to the one-dimensional Richards equation to simulate the water movement in unsaturated soils. This equation combines the mass balance and Darcy equations for unsaturated soils. The representation of the Richards equation is as follows (Eq. 1):

$$C(h)\frac{\partial h}{\partial t}=\frac{\partial}{\partial z}\left[K(h)\left(\frac{\partial h}{\partial z}+1\right)\right]-S_a(h) \qquad (1)$$

where: $C(h)$ is the slope of the soil-water retention curve (1/cm); h is the matric potential; t is the time elapsed (d); z is the elevation above the datum (cm); $K(h)$ is the unsaturated hydraulic conductivity (cm/d); and $S_a(h)$ represents the root uptake ($cm^3/cm^3.d$). The SWAP model utilizes the functions introduced by Van Genuchten (1980) and Mualem (1976) to characterize unsaturated soil water content and hydraulic conductivity (Eqs. 2-3):

$$\theta(h)=\theta_r+\frac{\theta_s-\theta_r}{(1+|\alpha h|^n)^{(n-1)/n}} \qquad (2)$$

$$K(\theta)=K_s S_e^{1/2}\left[1-(1-S_e^{n/(n-1)})^{(n-1)/n}\right]^2 \qquad (3)$$

where: θ_r, θ_s, and $\theta(h)$ are, respectively, the residual, saturated, and actual soil water contents (cm^3/cm^3); α (1/cm) and n (dimensionless) are shape parameters; $K(\theta)$ and K_s are, respectively, the unsaturated and saturated hydraulic conductivities (cm/d); and $S_e=(\theta_h-\theta_r)/(\theta_s-\theta_r)$. The soil hydraulic parameters in the SWAP model (θ_r, θ_s, K_s, α, and n) can be calibrated using the Parameter ESTimation (PEST) model. PEST, a widely used parameter estimation package, facilitates the calibration of hydrological models by employing various optimization algorithms (Li et al., 2017). For the current study, soil water content data from field measurements were employed to calibrate the above parameters. To accomplish this, the following objective function was minimized (Eq. 4):

$$\varphi(\theta,b)=\sum_{i=1}^{N}W_i\left[\theta_{obs}(z,t_i)-\theta_{sim}(z,t_i,\mathbf{b})\right]^2 \qquad (4)$$

where: **b** is the vector of parameters; $\theta_{obs}(z,t_i)$ is the measured water content at the depth z and the time t_i; $\theta_{sim}(z, t_i, \mathbf{b})$ is the corresponding simulated water content; N is the number of observations; and W_i is the weight coefficient of the ith observation. Finding a unique vector of parameters that minimizes the goal function is desired.

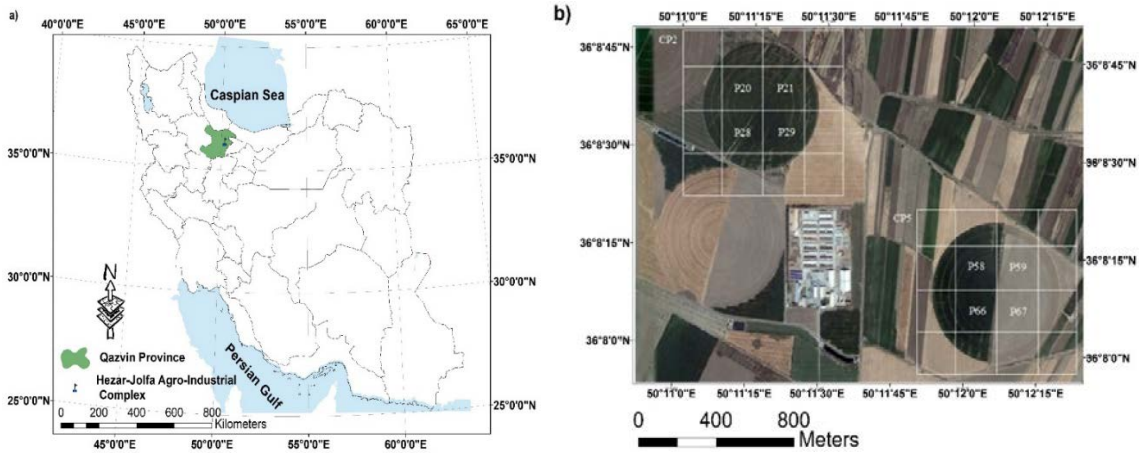

Fig. 1. Map of Iran and location of the study area (a); aerial photo of the fields under study and the location of measuring subsections (b)

The SWAP model comprises four input files: the primary input file, a meteorological data file, a file containing information about cultivated plants, and a file containing irrigation data. Daily weather information has been obtained from the nearest meteorological station to the region, specifically the Qazvin City synoptic station. This dataset includes daily records of minimum and maximum air temperatures, relative humidity, sunshine hours, and precipitation depths, covering the period from June 25, 2012, to October 15, 2012, representing the region's growing season.

Various crucial soil physical properties for the SWAP model include soil texture, soil organic matter, percentage of soil particles, and soil apparent particle density. On the eight square subsections within the CP2 and CP5 fields (Fig. 1), soil texture was determined through on-field measurements, the percentage of soil particles via the hydrometer method, apparent particle density using a core sampler, and the percentage of organic matter through an examination of previous studies in the Hezar-Jolfa Agro-Industrial Complex.

Irrigation data includes managerial parameters such as irrigation method, irrigation depth, irrigation frequency, and water quality. The CP2 and CP5 fields are irrigated using center-pivot irrigation systems. The data required for the irrigation section were derived from the rotation speed of the clockwise irrigation system and irrigation hours. During field sampling, it was observed that mechanized irrigation systems did not operate by the designated rotation and depth. Consequently, manual calibration of the irrigation calendar and depths was performed in the model's input.

Essential soil data for the model includes soil layering and hydraulic parameters of the Van Genuchten-Mualem functions. It is essential to highlight that the calibration of soil hydraulic parameters was executed using the PEST parameter estimation model. Iteratively, PEST minimizes the difference between observed and calculated data, resulting in error reduction and model calibration. For the calibration of soil hydraulic parameters, the inverse modeling was employed using PEST, which was integrated into the SWAP model. Parameter calibration was conducted for all square subsections (Fig. 1), defining an objective function to minimize the difference between observed water contents and simulated values by the SWAP model.

SWAP utilizes the Penman-Monteith equation to estimate potential ET, incorporating meteorological variables recorded at the Qazvin city synoptic station. ETa is then computed, considering soil water availability, crop resistance, and meteorological conditions. Throughout the calibration process, these parameters were fine-tuned to more accurately reflect the measured water content data obtained from the CP2 and CP5 fields. Ultimately, the ETa data served as a benchmark for evaluating the estimations provided by the SEBAL algorithm in the region.

The measured water content data spanned 18 days of the growing season in the region, from June 25, 2012, to October 15, 2012. As mentioned earlier, samples were extracted from depths of 0-15, and 15-30 cm at four randomly selected points within each square subsection depicted in Fig. 1. Soil water content measurement was conducted through soil sampling using the weight method, a common and practical technique employed in agriculture. Throughout an 18-day sampling period spanning the growing season, 144 (18 days × 4 squared subsections samples × 2 depths) were collected, and the water content of each sample was measured.

2.3. The SEBAL Algorithm

SEBAL stands as the extensively utilized algorithm for estimating regional ET through the utilization of remotely sensed data. By employing satellite-based data and the surface energy budget equation, SEBAL calculates the available energy flux at the surface, enabling the estimation of ET. The energy budget equation can be expressed in the following manner (Eq. 5):

$$LE = R_n - G - H \quad (5)$$

where: LE is the latent heat flux (W/m^2); R_n is the net radiation flux at the surface (W/m^2); G is the soil heat flux (W/m^2); and H is the sensible heat flux to the air (W/m^2). By utilizing the latent evaporation heat, the latent heat flux (LE) can be converted into the rate of ET.

The calculation of the net radiation flux at the surface (R_n) involves considering several factors, including the incoming shortwave radiation ($R_{S\downarrow}$), the surface albedo (α), the incoming longwave radiation ($R_{L\downarrow}$), the outgoing longwave radiation ($R_{L\uparrow}$, the sum of surface emitted and reflected atmospheric thermal radiation), and the surface thermal emissivity (ε_0) (Eq. 6):

$$R_n = (1 - \alpha)R_{S\downarrow} + R_{L\downarrow} - R_{L\uparrow} + (1 - \varepsilon_0)R_{L\downarrow} \quad (6)$$

where: $R_{S\downarrow}$, $R_{L\downarrow}$,, $R_{L\uparrow}$ are in W/m^2, and α and ε_0 are dimensionless. The soil heat flux (G) can be estimated empirically by considering the surface temperature, the surface albedo (α), and the Normalized Differential Vegetation Index (NDVI) as influencing factors.

The sensible heat flux can be computed using the physical characteristics of air, the aerodynamic resistance against heat transfer, and surface-to-air temperature difference. Details of the SEBAL algorithm can be found in Bastiaanssen et al. (1998b). The present study used the MATrix LABoratory (MATLAB) software and the Moderate Resolution Imaging Spectroradiometer (MODIS) products to implement the SEBAL algorithm in the study area.

2.4. Error measurements

The evaluation of the SWAP model's performance in simulating water content and the SEBAL algorithm's accuracy in estimating ET was conducted by assessing various metrics, including Root Mean Square Error (RMSE), coefficient of determination (R^2), Mean Absolute Error (MAE), and Coefficient of Residual Mass (CRM). The CRM metric indicates the model's inclination to overestimate or underestimate the measured values. A positive CRM suggests a tendency to overestimate, with a higher positive value indicating greater overestimation. Conversely, a negative CRM indicates an inclination to underestimate, and a more negative value reflects a higher degree of underestimation. RMSE, R^2, MAE, and CRM are defined as follows, respectively (Eqs. 7-10):

$$\mathrm{RMSE} = \sqrt{\frac{1}{N}\sum_{i=1}^{N}(M_i - S_i)^2} \tag{7}$$

$$\mathrm{R}^2 = \frac{\left[\sum_{i=1}^{N}\left(M_i - \bar{M}\right)\left(S_i - \bar{S}\right)\right]^2}{\sum_{i=1}^{N}\left(M_i - \bar{M}\right)^2 \sum_{i=1}^{N}\left(S_i - \bar{S}\right)^2} \tag{8}$$

$$\mathrm{MAE} = \frac{1}{N}\sum_{i=1}^{N}\left|M_i - S_i\right| \tag{9}$$

$$\mathrm{CRM} = 1 - \frac{\sum_{i=1}^{N} S_i}{\sum_{i=1}^{N} M_i} \tag{10}$$

where: N is the number of observations and $\bar{M}$ and $\bar{S}$ are, respectively, the mean of M_i (measured values) and S_i (simulated values). In the assessment of SWAP, M_i, and S_i are, respectively, the ith measured and simulated water contents; and in evaluating the performance of SEBAL, M_i is the ET simulated by the SWAP model, and S_i is the ET estimated by the SEBAL algorithm; The normalized RMSE (nRMSE), which is the ratio of RMSE to the mean of M_i values, was also calculated.

3. Results and discussion

The SWAP model was calibrated using the measured soil water content data at the CP2 field (see Fig. 1), and the optimal values for the soil hydraulic parameters were determined. Table 1 presents the optimal values of the parameters (θ_r, θ_s, K_s, α, and n). The performance of the SWAP model, calibrated with these values, was evaluated for estimating soil water content in the two studied fields using metrics such as RMSE, R^2, MAE, CRM, and nRMSE. Fig. 2 represents the mentioned error measure for both fields (CP2 and CP5) and in both soil layers.

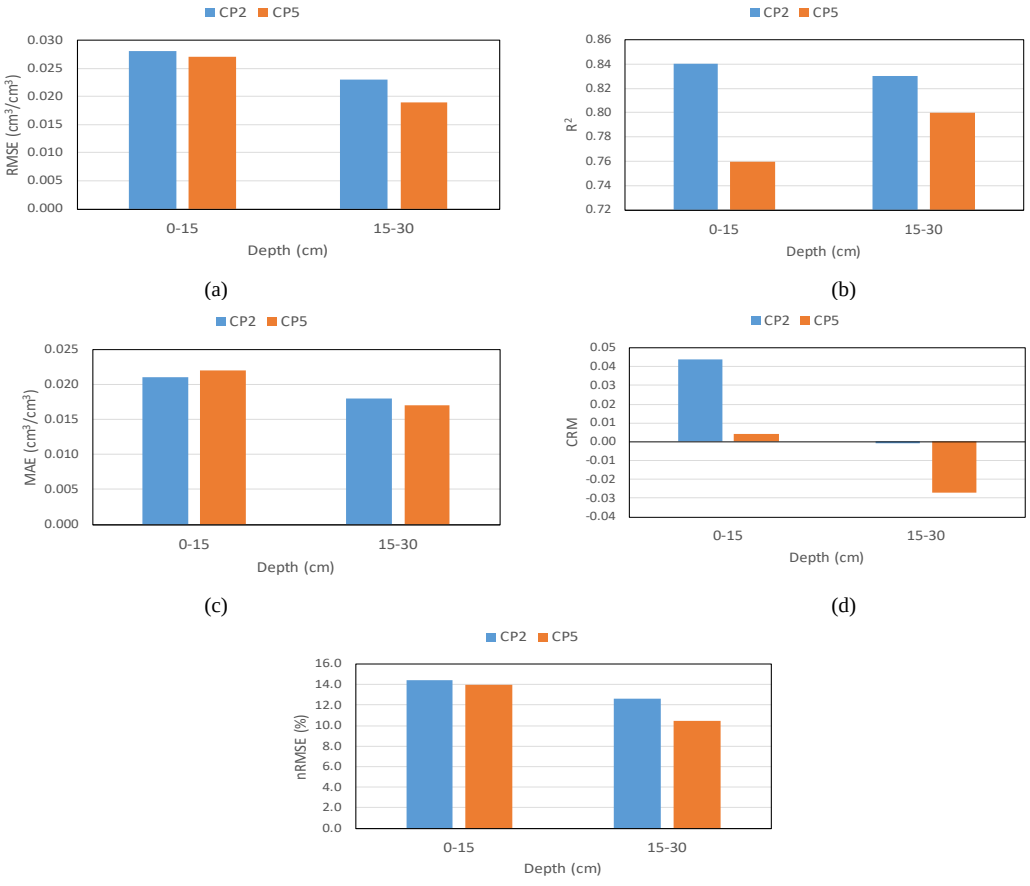

Fig. 2. Performance measures of the SWAP model in estimating soil water content for both fields under study (CP2 and CP5): (a) RMSE, (b) R^2, (c) MAE, (d) CRM, (e) n RMSE

Table 1. The optimum values of soil hydraulic parameters

Soil depth (cm)	θ_r *(cm³/cm³)*	θ_s *(cm³/cm³)*	K_s *(cm/d)*	*α (1/cm)*	*n (dimensionless)*
0-15	0.060	0.470	53.9	0.0098	1.49
15-30	0.095	0.450	12.3	0.0128	1.42

As Fig. 2 suggests, the calibrated model shows reasonable results with RMSE ≤ 0.028 cm^3/cm^3, $R^2 \geq 0.76$, MAE ≤ 0.022 cm^3/cm^3, -0.027 ≤ CRM ≤ 0.044, and nRMSE ≤ 14.4% in both soil layers (0-15, and 15-30 cm). However, it is seen that the model's performance in the second layer (15-30 cm) is, to some extent, better. According to the CRM values presented in Fig. 2, it is also seen that the model tends to underestimate water content in the first layer (0-15 cm), but negative CRMs in the second layer (15-30 cm) show an overall overestimation of water content in this layer.

Droogers et al. (2010) assessed the SWAP model in two wheat and cotton fields and reported 0.67 and 0.84 for the coefficient of determination. Ma et al. (2015) calibrated the SWAP model in three wheat and corn fields and reported RMSE values of 0.013, 0.022, and 0.047 $cm^3\ cm^{-3}$ for RMSE, and 12.8, 14.6, and 16.5% for nRMSE. Using the SWAP model, Wang et al. (2020) conducted a two-year field experiment in the Guanzhong Plain of Northwest China, focusing on the water dynamics of winter wheat under deficit irrigation. The experiment involved three irrigation levels (100%, 80%, and 60% of ETa) at four growth stages, with a control group receiving sufficient irrigation. The verification results demonstrated the accuracy of the SWAP model in simulating soil water content (average relative error < 21.66%, RMSE < 0.07 $cm^3\ cm^{-3}$).

Khoshsimaie Chenar et al. (2021) assessed the SWAP model's performance with three maize hybrids and varying irrigation water salinity in Iran. During validation, the model demonstrated practical water content estimation across three layers (0-20, 20-40, and 40-60 cm), yielding RMSE values of 0.03, 0.03, and 0.04 $cm^3\ cm^{-3}$, respectively. It accurately predicted soil salinity in the 0-20 cm layer (RMSE = 0.67 $cm^3\ cm^{-3}$), but its precision diminished with increasing depth (RMSE = 1.16 and 1.19 $cm^3\ cm^{-3}$ in the 20-40 and 40-60 cm layers).

Discrepancies arise when examining outcomes from other studies. Droogers et al. (2010) documented a lower coefficient of determination (0.67 and 0.84), contrasting with the high R^2 observed in our study. Further comparison with Ma et al. (2015) reveals variations in model performance, displaying different RMSE and nRMSE values for wheat and corn fields. These differences may be rooted in diverse environmental conditions, crop types, or specifics of model calibration procedures. Wang et al. (2020) study in the Guanzhong Plain offers a direct comparison, focusing on the water dynamics of winter wheat under deficit irrigation. Despite similarities in experimental setups, differences in RMSE values suggest potential variations in local factors influencing soil water dynamics. Comparing our results with those of Khoshsimaie Chenar et al. (2021), where the model had similar performance in all layers, reveals a discrepancy. In our study, however, the model exhibited improved performance in the second layer (15-30 cm), indicating variations in the model's behavior between the two studies. This contrast in model behavior suggests variations in factors influencing soil water dynamics between the two studies, potentially arising from different environmental conditions, calibration methodologies, or regional specifics.

In summary, while the conditions of each study may impact the accuracy of the results obtained from the model, comparing the statistical criteria of this study with the values obtained in previous studies demonstrates the model's satisfactory precision in soil moisture estimation. Consequently, the estimated ET rates by the model can be effectively utilized for evaluating the SEBAL algorithm.

MODIS products were used during the cropping season to estimate the input data for the SEBAL algorithm. For example, Fig. 3 shows the spatial distribution of NDVI, surface albedo, land surface temperature, sensible heat flux, and net radiation flux over the study area on September 22, 2012. The spatial resolution of the input data for the SEBAL algorithm, derived from MODIS products, is either 250 meters (NDVI, surface albedo, sensible heat flux, and net radiation flux) or 500 meters (land surface temperature). These data were used with the exact spatial resolution, and no downscaling was performed. In this figure., the locations of the two fields under study are also presented.

Figure 4 displays the temporal changes of the input data mentioned throughout the cropping season. Additionally, Fig. 5 illustrates the spatial distribution map of cumulative ETa across the study area, generated using the SEBAL algorithm.

Comparable maps were produced throughout the cropping season within the study area. Using the calibrated SWAP model, the ETa rates for both CP2 and CP5 fields were also estimated during cropping season. The scatter plot between all the ETa rates estimated by the SWAP model and the ones estimated by the SEBAL algorithms is shown in Fig. 6. As Fig. 6 suggests, there is a linear relationship between two data sets ($R^2 = 0.67$); however, the SEBAL algorithm has a clear tendency to underestimate ET_a. RMSE, R^2, MAE, CRM, and nRMSE values are also presented in Table 2. RMSE and nRMSE values are relatively high, suggesting the methods have different performances. A negative value of CRM shows that the values generated by SWBAL are generally greater than those generated by SWAP. Fig. 7 compares SEBAL and SWAP ET_a rates during cropping season. As it seen, the output of SEBAL for some days is zero, indicating

that the algorithm is not applicable on cloudy days. Fig. 6 suggests that SEBAL and SWAP follow a similar temporal pattern; however, the overestimation of SEBAL is apparent.

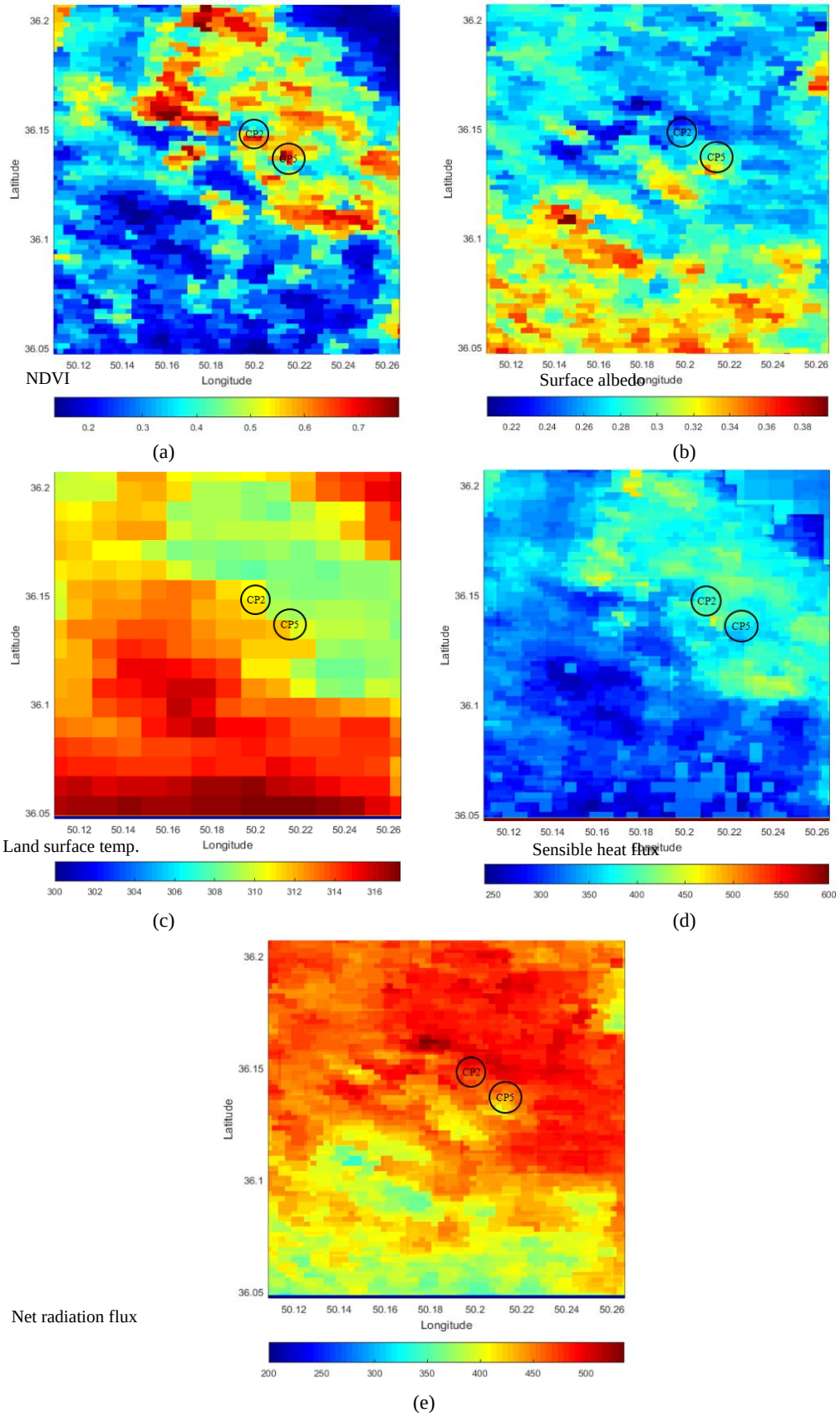

Fig. 3. Spatial pattern of surface albedo, land surface temperature (K), NDVI, sensible heat flux (W/m^2), and net radiation flux (W/m^2) over the study area on September 22, 2012: (a) NDVI, (b) Surface albedo, (c) Land surface temp., (d) Sensible heat flux, (e) Net radiation flux

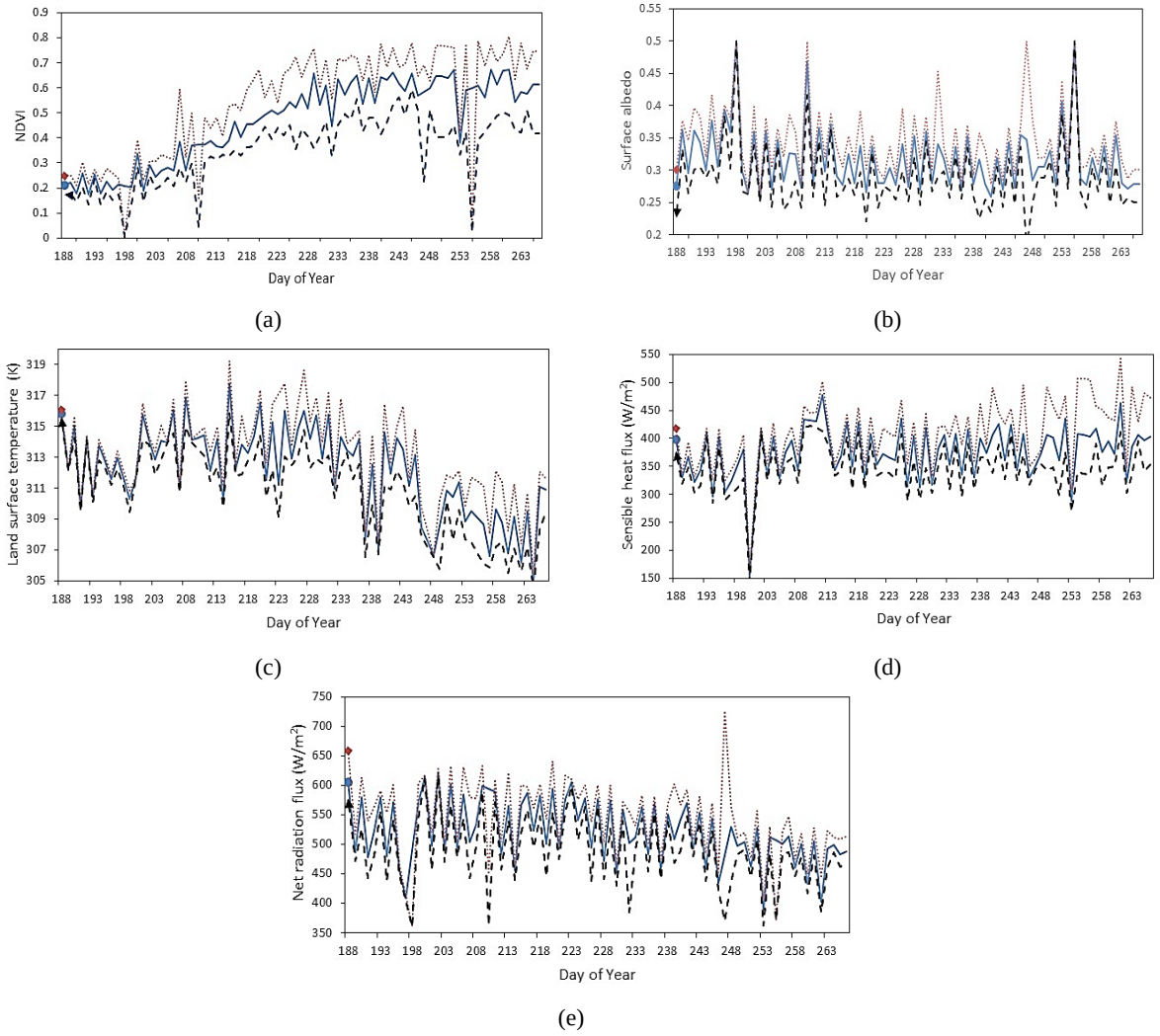

Fig. 4. Temporal variation of surface albedo, NDVI, land surface temperature, sensible heat flux, and net radiation in the study area over cropping season: (a) , (b) , (c) , (d) , (e)

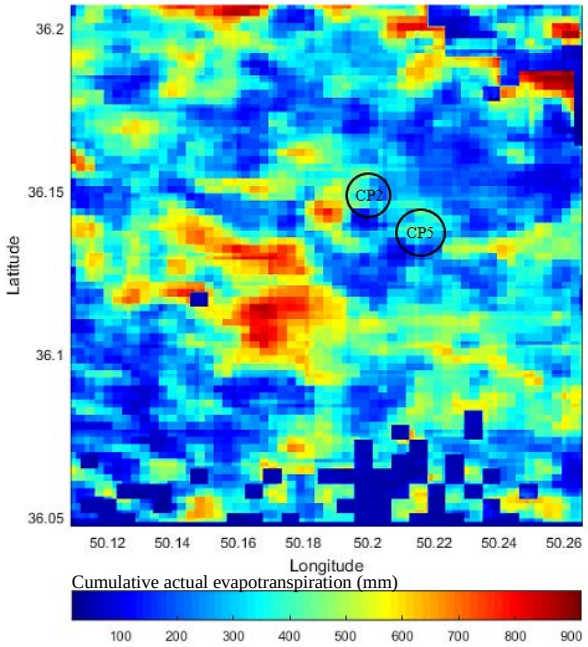

Fig. 5. Spatial pattern of cumulative ETa (mm) estimated by SEBAL over the study area

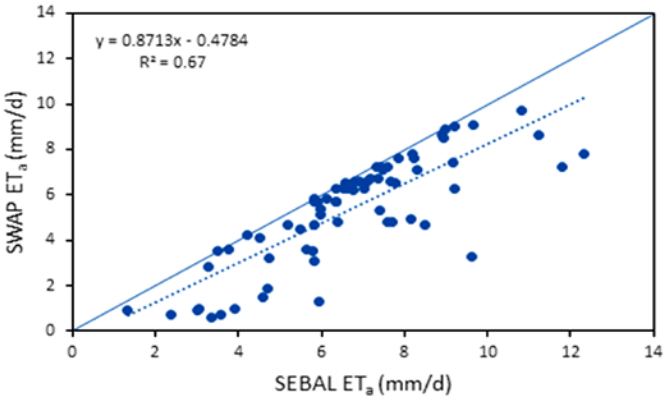

Fig. 6. Comparison between all ETa rates estimated using the SEBAL algorithm and the ones estimated by the calibrated SWAP model

Table 2. Summary statistics comparing the overall performance of SEBAL in comparison to the SWAP model

RMSE (mm/day)	*R^2*	*MAE*	*CRM*	*nRMSE (%)*
2.3	0.67	0.937	-0.139	44.2

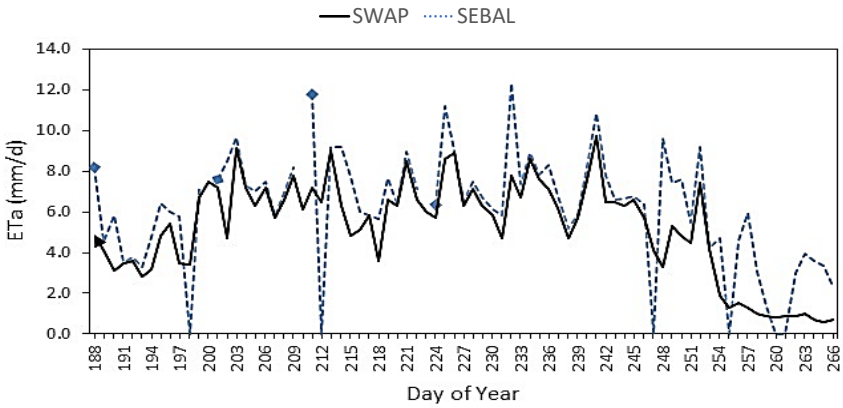

Fig. 7. Comparison between the temporal variations of ETa rates estimated using the SEBAL algorithm and the ones estimated by the calibrated SWAP model

Awada et al. (2021) utilized the SEBAL model on Landsat images (2009-2014) over a Mediterranean maquis in Sardinia, Italy. Comparing SEBAL with tower data indicated robust estimations (R^2 = 0.77, RMSE = 0.05, MAE = 0.076). Their conclusion supported SEBAL's satisfactory performance, emphasizing its potential to understand ET dynamics in complex ecosystems for broader environmental and hydrological applications. In a separate study, Chen et al. (2023) applied SEBAL in the Shiyang River Basin, northwest China, for the 2020 growing season. Results demonstrated a good correlation with Penman-Monteith-derived data (R^2 = 0.85) but noted slight overestimation compared to MODIS ET. Ma et al. (2023) proposed Y-SEBAL, a surface energy balance model built upon SEBAL with improved sensible heat flux calculation. The introduction of an empirical formula for sensible heat flux in Y-SEBAL addresses limitations present in SEBAL. The researchers demonstrated the model's efficacy in accurately simulating regional ET, validated against eddy covariance data (R = 0.82, agreement index = 0.90, RMSE = 0.81 mm·d^{-1}). Their conclusion highlights Y-SEBAL's capacity to enhance simulation performance, presenting a novel remote sensing-based regional ET retrieval solution.

The observed differences in estimating ETa among studies can be attributed to several key factors. Firstly, environmental variability plays a crucial role, as studies are often conducted in diverse geographical locations with distinct climates, soil types, and overall environmental conditions. These variations introduce unique challenges for the models in capturing the local intricacies of water dynamics. Secondly, the types of crops and land cover present in the study areas contribute to disparities. Different vegetation types and land cover characteristics have distinct impacts on the energy and water balance, influencing the accuracy of models in estimating ET.

Furthermore, variations in model calibration procedures add another layer of complexity. Calibration involves adjusting model parameters to align with observed data. Differences in calibration methods, the quality of input data, and the specificities of the calibration process can contribute to variations in model performance across studies.

The benchmark employed in the present study for evaluating ETa rates is derived from a calibrated

SWAP model. It is crucial to note that this differs from benchmarks used in other studies, such as Awada et al. (2021) utilizing tower data in a Mediterranean maquis in Sardinia, Italy, and Chen et al. (2023) using Penman-Monteith-derived data in the Shiyang River Basin, northwest China. Whether model-derived or measured through alternative methods, the choice of benchmarks introduces variations in the comparative assessment of model performance. These discrepancies highlight the importance of considering the specific benchmark sources and methodologies when interpreting and comparing results across different studies. Considering these factors, it becomes evident that the differences in environmental conditions, land cover, and calibration approaches collectively contribute to the differences observed in the results of studies utilizing models like SWAP and SEBAL for estimating ETa.

4. Conclusions

The primary inquiry of this study was whether remote sensing-derived ETa data can be confidently applied for agricultural irrigation planning and management. Addressing this question and evaluating the ETa derived from remote sensing requires assessing these data against a ground truth benchmark. In this study, due to the absence of lysimeter data on ETA in the study area (the Hezar-Jolfa Agro-Industrial Complex, Qazvin, Iran), the SWAP model was utilized to obtain accurate data on ETa. Initially, this model was validated using observational data on soil moisture. Given the model's precision in estimating soil moisture, it was concluded that the ETa derived from the SWAP model can be considered a suitable benchmark.

The SWAP model demonstrated satisfactory precision in estimating soil moisture content across different soil layers through calibration and validation processes. The study established the model's credibility in simulating soil water dynamics in the region by comparing error metrics such as RMSE, R2, MAE, CRM, and nRMSE with those reported in previous studies. Despite tending to underestimate ETa, the SEBAL algorithm's performance was assessed against the calibrated SWAP model, revealing a linear relationship between the two datasets. The R^2 value between ETa from SWAP and SEBAL was calculated as 0.67, indicating a moderate level of correlation between the two methods.

One of the limitations of this study has been the constraint related to ground data acquisition. Additionally, in some instances where ground data were available, due to the cloudy weather conditions in the study area, SEBAL may not have performed optimally.

Considering the advantages of remote sensing data, such as high spatial resolution and ease of access, assessing other existing methods for extracting ETa from remote sensing measurements and comparing them with SEBAL could be a significant topic for future studies. These evaluations can contribute to examining the accuracy, precision, and reliability of various methods in estimating ETa.

References

Allen R.G., Tasumi M., Morse A., Trezza R., (2005), A Landsat-based energy balance and evapotranspiration model in Western US water rights regulation and planning, *Irrigation and Drainage Systems*, **19**, 251-268.

Anderson M.C., Norman J.M., Diak G.R., Kustas W.P., Mecikalski J.R., (1997), A two-source time-integrated model for estimating surface fluxes using thermal infrared remote sensing, *Remote Sensing of Environment*, **60**, 195-216.

Awada H., Di Prima S., Sirca C., Giadrossich F., Marras S., Spano D., Pirastru M., (2021), Daily actual evapotranspiration estimation in a Mediterranean ecosystem from landsat observations using SEBAL approach, *Forests*, https://doi.org/10.3390/f12020189.

Badiehneshin A., Noory H., Vazifedoust M., (2015), Improving crop yield estimation through SWAP model using satellite data, *Iranian Journal of Soil and Water Research*, **45**, 379-388.

Bastiaanssen W.G.M., Menenti M., Feddes R.A., Holtslag A.A.M., (1998a), A remote sensing surface energy balance algorithm for land (SEBAL). 1. Formulation, *Journal of Hydrology*, **212-213**, 198-212, https://doi.org/10.1016/S0022-1694(98)00253-4

Bastiaanssen W.G.M., Pelgrum H., Wang J., Ma Y., Moreno J.F., Roerink G.J., van der Wal T., (1998b), A remote sensing surface energy balance algorithm for land (SEBAL). 2. Validation, *Journal of Hydrology*, **212-213**, 213-229, https://doi.org/10.1016/S0022-1694(98)00254-6

Bennett S.J., Bishop T.F.A., Vervoort R.W., (2013), Using SWAP to quantify space and time related uncertainty in deep drainage model estimates: A case study from northern NSW, Australia, *Agricltural Water Managment*, **130**, 142-153.

Chen X., Yu S., Zhang H., Li F., Liang C., Wang Z., (2023), Estimating the actual evapotranspiration using remote sensing and SEBAL model in an arid environment of northwest China, *Water*, https://doi.org/10.3390/w15081555.

Droogers P., Immerzeel W.W., Lorite I.J., (2010), Estimating actual irrigation application by remotely sensed evapotranspiration observations, *Agricultural Water Management*, **97**, 1351-1359, https://doi.org/https://doi.org/10.1016/j.agwat.2010.03.017

Fallah M., (2014), *Estimation of soil moisture using the agrohydrological SWAP model and its comparison with field and satellite soil moisture data*, MSc Thesis, University of Guilan, Rasht, Iran.

Faraji Z., Kaviani A., Ashrafzadeh A., (2017), Assessment of GRACE satellite data for estimating the groundwater level changes in Qazvin province, *Iranian Journal of Ecohydrology*, **4**, 463-476, https://doi.org/10.22059/ije.2017.61482.

Foster T., Mieno T., Brozović N., (2020), Satellite-based monitoring of irrigation water use: Assessing measurement errors and their implications for agricultural water management policy, *Water Resources Research*, https://doi.org/https://doi.org/10.1029/2020WR028378

Gandolfi C., Facchi A., Maggi D., (2006), Comparison of 1D models of water flow in unsaturated soils. *Environmental Modeling & Softwar*e, **21**, 1759-1764,

https://doi.org/https://doi.org/10.1016/j.envsoft.2006.04.004.

Gebremedhin M.A., Lubczynski M.W., Maathuis B.H.P., Teka D., (2022), Deriving potential evapotranspiration from satellite-based reference evapotranspiration, Upper Tekeze Basin, Northern Ethiopia, *Journal of Hydrology Regional Studies*, **41**, 101059, https://doi.org/10.1016/j.ejrh.2022.101059.

Ghiat I., Mackey H.R., Al-Ansari T., (2021), A review of evapotranspiration measurement models, techniques and methods for open and closed agricultural field applications, *Water*, **13**, 2523 https://doi.org/10.3390/w13182523.

Giles-Hansen K., Wei X., (2021), Improved regional scale dynamic evapotranspiration estimation under changing vegetation and climate, *Water Resources Research*, **57**, e2021WR029832, https://doi.org/https://doi.org/10.1029/2021WR029832

Hassanli M., Ebrahimian H., Mohammadi E., Rahimi A., Shokouhi A., (2016), Simulating maize yields when irrigating with saline water, using the AquaCrop, SALTMED, and SWAP models, *Agricltural Water Managment*, **176**, 91-99.

Khoshsimaie Chenar M., Noory H., Mahmoudi Molamahmoud Z., (2021), Evaluation of SWAP model in estimating soil water content, salinity and yield of three forage maize cultivars under saline water use conditions (in Persian), *Journal of Water and Irrigation Management*, **11**, 495-512.

Kim J., Mohanty B.P., Shin Y., (2015), Effective soil moisture estimate and its uncertainty using multimodel simulation based on Bayesian Model Averaging, *Journal of Geophysical Research: Atmospheres*, 120, 8023-8042.

Kottek M., Grieser J., Beck C., Rudolf B., Rubel F., (2006), World map of the Köppen-Geiger climate classification updated. Meteorol, *Zeitschrift*, **15**, 259-263.

Kumar P., Sarangi A., Singh D.K., Parihar S.S., Sahoo R.N., (2015), Simulation of salt dynamics in the root zone and yield of wheat crop under irrigated saline regimes using SWAP model, *Agricltural Water Managment*, **148**, 72-83.

Li N., Sun Y., Wan L., Ren L., (2017), Estimating soil hydraulic parameters by inverse modeling with PEST, *Vadose Zone Journal*, **16**, https://doi.org/10.2136/vzj2017.02.0042.

Li Z.-L., Tang R., Wan Z., Bi Y., Zhou C., Tang B., Yan G., Zhang X., (2009), A review of current methodologies for regional evapotranspiration estimation from remotely sensed data, *Sensors*, **9**, 38-53

Ma Y., Feng S., Song X., (2015), Evaluation of optimal irrigation scheduling and groundwater recharge at representative sites in the North China Plain with SWAP model and field experiments, *Computers and Electronics in Agriculture*, **116**, 125-136.

Ma Y., Sun S., Li C., Zhao J., Li Z., Jia C., (2023), Estimation of regional actual evapotranspiration based on the improved SEBAL model, *Journal of Hydrology*, **619**, 129283.

Minacapilli M., Agnese C., Blanda F., Cammalleri C., Ciraolo G., D'Urso G., Iovino M., Pumo D., Provenzano G., Rallo G., (2009), Estimation of actual evapotranspiration of Mediterranean perennial crops by means of remote-sensing based surface energy balance models, *Hydrology and Earth System Sciences*, **13**, 1061-1074.

Monteiro dos Reis M.A., Chioderoli C.A., da Silva A.O., (2022), Economic viability of different sweet corn production systems, *Environmental Engineering and Management Journal*, **21**, 707-713.

Noory H., Van Der Zee S.E.A.T.M., Liaghat A.M., Parsinejad M., van Dam J.C., (2011), Distributed agro-hydrological modeling with SWAP to improve water and salt management of the Voshmgir Irrigation and Drainage Network in Northern Iran, *Agricultural Water Managment*, **98**, 1062-1070.

Norman J.M., Kustas W.P., Humes K.S., (1995), Source approach for estimating soil and vegetation energy fluxes in observations of directional radiometric surface temperature, *Agricultural and Forest Meteorology*, **77**, 263-293.

Paul G., Gowda P.H., Vara Prasad P.V., Howell T.A., Staggenborg S.A., Neale C.M.U., (2013), Lysimetric evaluation of SEBAL using high resolution airborne imagery from BEAREX08, *Advances in Water Resources*, **59**, 157-168.

Su Z., (2002), The Surface Energy Balance System (SEBS) for estimation of turbulent heat fluxes, *Hydrology and Earth System Sciences*, **6**, 85-100.

Sun Z., Wei B., Su W., Shen W., Wang C., You D., Liu Z., (2011), Evapotranspiration estimation based on the SEBAL model in the Nansi Lake Wetland of China, *Mathematical and Computer Modelling*, **54**, 1086-1092.

van Dam J.C., de Rooij G., Heinen M., Stagnitti F., (2004), *Concepts and dimensionality in modeling unsaturated water flow and solute transport*, In: *Unsaturated-zone modeling; progress, challenges and applications*, Feddes R.A., de Rooij G.H., van Dam J.C. (Eds.), *Kluwer, Dordrecht*, 1-36.

Wang X., Cai H., Li L., Wang X., (2020), Estimating soil water content and evapotranspiration of winter wheat under deficit irrigation based on SWAP Model,. *Sustainability*, **12**, 9451, https://doi.org/10.3390/su12229451.

Wanniarachchi S., Sarukkalige R., (2022), A review on evapotranspiration estimation in agricultural water management: Past, present, and future, *Hydrology*, **9**, 123.

Wu B., Zhu W., Yan N., Xing Q., Xu J., Ma Z., Wang L., (2020), Regional actual evapotranspiration estimation with land and meteorological variables derived from multi-source satellite data, *Remote Sensing*, **12**, 332, https://doi.org/10.3390/rs12020332.

Zhou X., Bi S., Yang Y., Tian F., Ren D., (2014), Comparison of ET estimations by the three-temperature model, SEBAL model and eddy covariance observations, *Journal of Hydrology*, **519**, 769-776.